



University of  
**Salford**  
MANCHESTER

# Neutron diffraction studies of magnetostrictive Fe–Ga alloy ribbons

Zhao, X, Mellors, NJ, Kilcoyne, SH, Lord, DG, Lupu, N, Horia, C and  
Henry, P

<http://dx.doi.org/10.1063/1.2837244>

<b>Title</b>	Neutron diffraction studies of magnetostrictive Fe–Ga alloy ribbons
<b>Authors</b>	Zhao, X, Mellors, NJ, Kilcoyne, SH, Lord, DG, Lupu, N, Horia, C and Henry, P
<b>Type</b>	Article
<b>URL</b>	This version is available at: <a href="http://usir.salford.ac.uk/id/eprint/20744/">http://usir.salford.ac.uk/id/eprint/20744/</a>
<b>Published Date</b>	2008

USIR is a digital collection of the research output of the University of Salford. Where copyright permits, full text material held in the repository is made freely available online and can be read, downloaded and copied for non-commercial private study or research purposes. Please check the manuscript for any further copyright restrictions.

For more information, including our policy and submission procedure, please contact the Repository Team at: [usir@salford.ac.uk](mailto:usir@salford.ac.uk).



## Neutron diffraction studies of magnetostrictive Fe–Ga alloy ribbons

Xuegen Zhao, Nigel Mellors, Susan Kilcoyne, Don Lord, Nicoleta Lupu et al.

Citation: *J. Appl. Phys.* **103**, 07B320 (2008); doi: 10.1063/1.2837244

View online: <http://dx.doi.org/10.1063/1.2837244>

View Table of Contents: <http://jap.aip.org/resource/1/JAPIAU/v103/i7>

Published by the [American Institute of Physics](#).

---

### Related Articles

Magnetic and calorimetric studies of magnetocaloric effect in  $\text{La}_{0.7-x}\text{Pr}_x\text{Ca}_{0.3}\text{MnO}_3$

*J. Appl. Phys.* **111**, 07D726 (2012)

Converse magnetoelectric effect dependence with CoFeB composition in ferromagnetic/piezoelectric composites

*J. Appl. Phys.* **111**, 07C725 (2012)

A model-assisted technique for characterization of in-plane magnetic anisotropy

*J. Appl. Phys.* **111**, 07E344 (2012)

Magnetostriction measurement of a giant magnetoresistance film on a practical substrate covered by a shield layer

*J. Appl. Phys.* **111**, 07E340 (2012)

Dynamic magnetoelastic properties of epoxy-bonded  $\text{Sm}_{0.88}\text{Nd}_{0.12}\text{Fe}_{1.93}$  pseudo-1-3 negative magnetostrictive particulate composite

*J. Appl. Phys.* **111**, 07A940 (2012)

---

### Additional information on *J. Appl. Phys.*

Journal Homepage: <http://jap.aip.org/>

Journal Information: [http://jap.aip.org/about/about\\_the\\_journal](http://jap.aip.org/about/about_the_journal)

Top downloads: [http://jap.aip.org/features/most\\_downloaded](http://jap.aip.org/features/most_downloaded)

Information for Authors: <http://jap.aip.org/authors>

## ADVERTISEMENT



**FIND THE NEEDLE IN THE  
HIRING HAYSTACK**

Post jobs and reach  
thousands of hard-to-find  
scientists with specific skills



<http://careers.physicstoday.org/post.cfm> **physicstoday JOBS**

## Neutron diffraction studies of magnetostrictive Fe–Ga alloy ribbons

Xuegen Zhao,<sup>a)</sup> Nigel Mellors, Susan Kilcoyne, and Don Lord  
*Institute for Materials Research, University of Salford, Salford M5 4WT, United Kingdom*

Nicoleta Lupu and Horia Chiriac  
*National Institute of Research and Development for Technical Physics, Iasi 700050, Romania*

Paul F. Henry  
*Institut Laue-Langevin, F-38042 Grenoble, France*

(Presented on 7 November 2007; received 12 September 2007; accepted 7 November 2007; published online 1 February 2008)

Melt-spun Fe–Ga ribbons were prepared and some ribbons were annealed at 1000 °C for 1 h then slowly cooled to room temperature. X-ray diffraction patterns revealed no evidence of texture and only bcc phase in the as-quenched ribbons. However, high-resolution neutron diffraction patterns gave more information on the structure of these ribbons. Only diffractions from the disordered bcc A2 phase were found in as-quenched ribbons with 15, 17.5, and 19.5 at. % Ga content, without any trace of satellite peaks or splitting peaks from the proposed Ga–Ga pairing superlattice structure. The broadening of the base of the (110) peaks for all samples except the as-quenched 15 at. % Ga ribbon might indicate the existence of some kind of short range ordering. Ribbons developed  $L1_2$  phase after annealing especially in the Fe 19.5 at. % Ga ribbon where the formation of  $L1_2$  phase reduced the Ga content in the remaining A2 phase and decreased its lattice parameter dramatically.  $DO_3$  phase formed in the as-quenched 22.5 at. % Ga ribbon and the following annealing treatment transformed more A2 phase into  $DO_3$  phase. © 2008 American Institute of Physics.  
 [DOI: 10.1063/1.2837244]

### I. INTRODUCTION

The Fe–Ga system is characterized by a large solid solubility of Ga in bcc  $\alpha$ -Fe, 11 at. % at room temperature, and up to 36 at. % at 1037 °C.<sup>1</sup> However, appreciable amounts of Ga well in excess of the solubility limit can be retained in the metastable disordered bcc solid solution phase (A2 phase) at room temperature by rapid cooling.<sup>1–3</sup> The replacement of Fe by Ga results in a large increase in magnetostriction, approaching 400 ppm for quenched single crystals<sup>4–6</sup> at room temperature, with low saturation fields of several hundreds of oersted, and over –2000 ppm has been reported for melt-spun Fe–Ga ribbons.<sup>7,8</sup> The magnetostriction  $\lambda_{100}$  maximizes around 17–19 at. % of Ga and then decreases with increased Ga content.<sup>9</sup> The decrease of  $\lambda_{100}$  at higher Ga content coincides with the change of structure from the disordered bcc to a low-energy long range ordered phase ( $DO_3$ ). Local short-range ordering of the Ga atoms along the [100] direction in the disordered Fe structure has been suggested to be responsible for this increase<sup>10</sup> but experimental confirmation still remains a challenge.<sup>11,12</sup> This is because the peaks corresponding to both  $DO_3$  and A2 phases overlap except for the weak satellite peaks corresponding to the ordered structure. These satellite peaks can generally not be clearly identified due to the very low relative intensities found using x-ray diffraction. Neutron diffraction is expected to give better results as the difference in atomic scattering factor between Fe and Ga atoms is bigger in neutron diffraction and the atomic scattering factor does not change with the changing scanning angle.<sup>13</sup>

In this paper, we have studied the extent to which the disordered bcc phase can be retained at room temperature by melt spinning in the hope of further increasing  $\lambda_{100}$ . Neutron diffraction has been used to identify the  $DO_3$  phase and confirm the existence of possible short range order.

### II. EXPERIMENT

Ingots of  $Fe_{100-x}Ga_x$  ( $x=15, 17.5, 19.5, 21,$  and  $22.5$ ) were prepared by arc melting high purity (>99.9) constituent elements multiple times to ensure homogeneity. High vapor pressure of Ga and the use of care in the melting procedures resulted in negligible Ga loss. Ribbon samples were produced by melting 3 g of ingot with an induction coil in a partial argon atmosphere and ejecting the melt onto a rotating copper wheel at a wheel speed of 35 m/s. The orifice diameter of the quartz crucible was approximately 0.5 mm. Isothermal heat treatment was performed on some ribbons at 1000 °C for 1 h followed by slow cooling to room temperature. Ribbons were evacuated in a quartz tube and then sealed under approximately 1 atm of argon before heat treatment.

X-ray diffraction examinations were performed using a Bruker D8 Advance diffractometer. The  $\theta$ - $2\theta$  scans were obtained using  $Cu K\alpha$  radiation in a Bragg–Brentano configuration. The x-ray diffraction patterns obtained were used to determine the phases present and the crystallographic texture of the samples.

Neutron diffraction experiments were carried out on both as-quenched and annealed  $Fe_{100-x}Ga_x$  ( $x=15, 17.5, 19.5,$  and  $22.5$ ) alloy ribbons on the D2B diffractometer, ILL at

<sup>a)</sup>Electronic mail: x.zhao@salford.ac.uk.

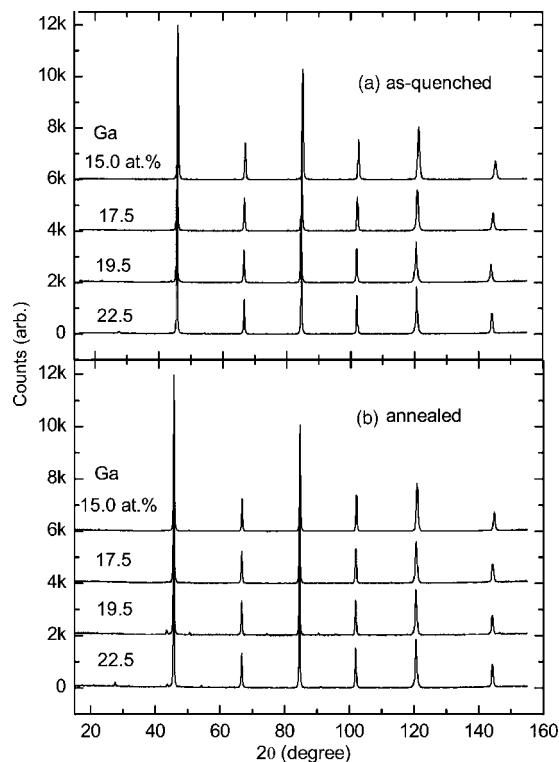


FIG. 1. Neutron diffraction patterns of as-quenched and annealed Fe-Ga ribbons.

Grenoble, France. Ribbon samples were packed into vanadium cans and scanned from  $0^\circ$  to  $158^\circ$  at ambient temperature by using the high-resolution mode with a scanning step size of  $0.05^\circ$ .

### III. RESULTS AND DISCUSSION

The x-ray diffraction patterns of as-quenched melt-spun ribbons show no evidence of obvious texture. In addition to the primary reflections at  $2\theta \sim 44^\circ$  (110) and  $\sim 64^\circ$  (200), no reflections corresponding to the  $DO_3$  phase were observed.

The neutron diffraction patterns from both melt-spun ribbons and annealed ribbons are shown in Fig. 1. The six strong diffraction peaks can be easily identified as arising from (110), (200), (211), (220), (310), and (222) reflections from the bcc ( $A_2$  phase) structure or correspondingly (220), (400), (422), (620), and (444) reflections from the  $DO_3$  structure. The ratios of peaks compared with the strongest diffraction peak [(110) for  $A_2$  phase or (220) for  $DO_3$  phase] intensities are almost identical among samples.

However, after enlarging the low intensity part of the diffraction patterns, as shown in Fig. 2, we can see some weak diffraction peaks, in addition to the six strong peaks. One group of them belongs to the vanadium container used in the experiment. Vanadium, being bcc with  $a=3.0297 \text{ \AA}$ , has diffraction peaks close to the left of  $A_2$  peaks and are clearly shown in the diffraction pattern of Fe 15 at. % Ga melt-spun ribbon. When the Ga content is increased to 22.5 at. %, extra peaks from the ordered  $Fe_3Ga DO_3$  structure are observed.

It is mentioned in several papers that Ga-Ga pairs formed along the  $\langle 100 \rangle$  direction may be responsible for the

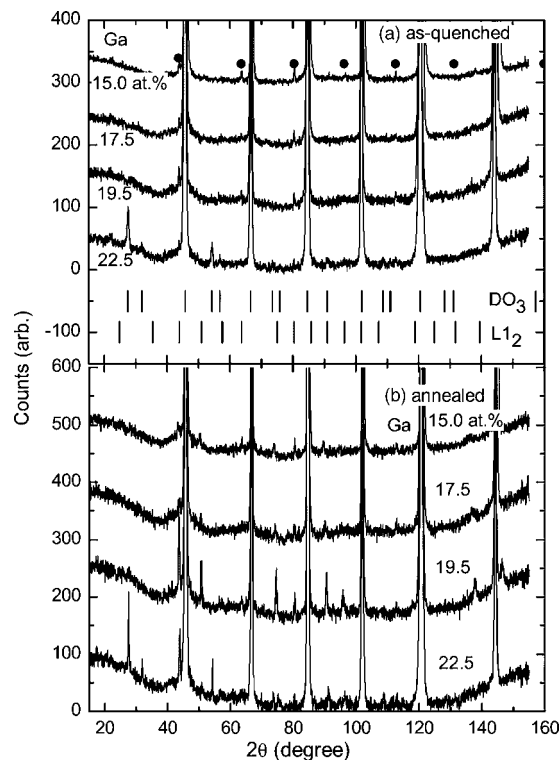


FIG. 2. Enlargement of the low intensity parts of Fig. 1. Peak positions of vanadium (●),  $DO_3$  and  $L_{12}$  phases are also shown.

high magnetostriction found in Fe-Ga alloys. This kind of ordering results in a structure change from bcc to tetragonal and should give some satellite peaks or even peak splitting.<sup>11</sup> These peaks are not expected to be identified from the  $DO_3$  phase as they will overlap. However, we cannot see any satellite peaks from such a superlattice structure or a noticeable splitting of the observed peaks for ribbons with 15, 17.5, and 19.5 at. % Ga, although these ribbons show only disordered  $A_2$  phase. Broadening of the base of the (110) peak for all samples except the as-quenched 15 at. % Ga ribbon might indicate the existence of some kind of short range ordering, although the possibility of thermal diffuse scattering from phonons could not be excluded considering that the dramatic elastic softening occurs in these materials with Ga doping.<sup>14</sup>

More peaks were observed in the patterns from samples which had been annealed at  $1000^\circ\text{C}$  for 1 h then slowly cooled down to room temperature, especially with  $x = 19.5$  at. % Ga. These new peaks have been indexed as coming from a  $Fe_3Ga L_{12}$  phase. It was a surprise to observe this phase appearing in these annealed ribbon samples as it is believed that the  $L_{12}$  phase is very difficult to form and we have not seen such a phase in annealed Fe-Ga bulk samples. However, this annealing treatment has not developed a significant volume of the  $DO_3$  phase in the 19.5 at. % Ga ribbon and no obvious Bragg peaks from  $DO_3$  can be seen even in the low intensity part of the diffraction pattern. This may indicate a structural transformation from  $A_2$  to  $L_{12}$ , rather than from  $DO_3$  to  $L_{12}$  during the annealing process.

It is difficult to tell how much  $A_2$  phase exists in the 22.5 at. % Ga ribbons. No obvious peak splitting can be seen with the peaks above  $60^\circ$ , in fact, they can be easily fitted with a single-peak profile. However, the percentage of the

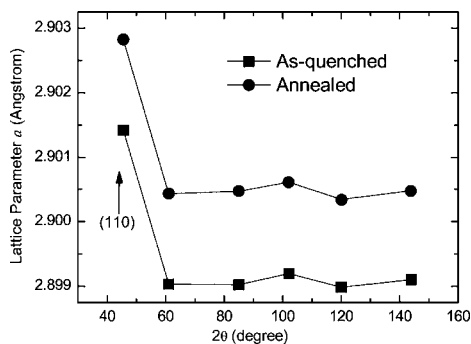


FIG. 3. Lattice parameters fitted from individual diffraction peaks of Fe 17.5 at. % ribbons.

$DO_3$  superlattice peak intensities at  $2\theta \sim 27.5^\circ$  and  $57.2^\circ$  compared with the (220) peak, increases from 1% and 0.5% to 2.4% and 1%, respectively, after annealing, within an uncertainty of  $\pm 0.3\%$ . This increase in intensity seems to indicate an increase in the volume of  $DO_3$  phase after annealing, which in turn implies that there might be A2 phase in the as-quenched ribbons and some A2 phase be transformed into  $DO_3$  phase after annealing.

To calculate the lattice parameters, we fitted the diffraction patterns with GSAS, a software package for diffraction refinement.<sup>15</sup> It has been noticed that the low angle (110) peak is different from all other peaks and cannot be treated as a simple single peak. The lattice parameters calculated from individual peaks from the Fe 17.5 at. % Ga ribbon are shown in Fig. 3. Clearly, the (110) peak produces a parameter well above the average. Although these ribbons are ferromagnetic materials and there are both magnetic and structural contributions to this peak, the magnetic peak is at the same position as the structural one, and should not affect the calculation of the lattice parameters. The cause of this abnormal value is still under investigation.

By assuming a bcc (A2) structure and only using three high angle peaks to avoid the possible error resulting from the low angle (110) peaks, the calculated parameter  $a$  values are shown in Fig. 4. The  $DO_3$  structure has a lattice parameter of  $2a$ .

With the increase in Ga content, the structure of the ribbons changes from disordered bcc for 19.5 at. % to ordered-bcc structure for 22.5 at. %, which results in a decrease in lattice parameters as expected.<sup>16,17</sup>

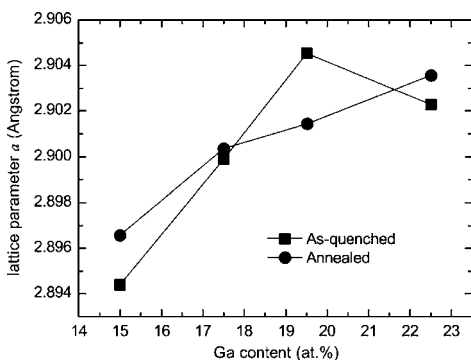


FIG. 4. Lattice parameters of as-quenched and annealed ribbons.

It can be seen from Fig. 4 that the ribbon sample with 19.5 at. % Ga shows a significant change in lattice parameter after annealing treatment. The as-quenched ribbon has A2 phase with  $a = 2.9045 \text{ \AA}$ . After heat treatment, the ribbon has developed ordered  $L1_2 \text{ Fe}_3\text{Ga}$  phase and possibly  $DO_3 \text{ Fe}_3\text{Ga}$  phase as well that reduce the Ga content in the A2 phase and, thus, the lattice parameter reduces down to  $2.9014 \text{ \AA}$ . Using this parameter and the relation between composition and lattice parameter obtained from the annealed ribbons with 15 and 17.5 at. % Ga, it is estimated that the annealed 19.5 at. % ribbon might have an actual Ga content of 18.1 at. % for the A2 phase, and the volume fraction of  $L1_2$  phase could be around 20%.

Both  $DO_3$  and  $L1_2 \text{ Fe}_3\text{Ga}$  phases have different magnetic properties to disordered A2 Fe–Ga alloys, and will therefore act as impurities in the A2 matrix, such as rare-earth inclusions in Terfenol-D, decreasing the magnetostrictive performance of the materials. If element ( $M$ ) substitution or the addition method, in addition to quenching, can be used to hinder the formation of second phase material such as  $DO_3$  while still maintaining a high Ga content and high Curie temperature, then it may be possible to obtain much higher magnetostriction from Fe–Ga– $M$  alloys.

## ACKNOWLEDGMENTS

This work was generated in the context of the MESEMA project, funded under the 6th Framework Programme of the European Community (Contract No. AST3-CT-2003-502915).

- <sup>1</sup>H. Okamoto, in *Phase Diagrams of Binary Iron Alloys*, Monograph Series on Alloy Phase Diagrams No. 9, edited by H. Okamoto (ASM International, Materials Park, OH, 1993), pp. 147–151
- <sup>2</sup>C. Dasarthy and W. Hume-Rothery, *Proc. R. Soc. London, Ser. A* **286**, 141 (1965).
- <sup>3</sup>H. L. Luo, *Trans. Metall. Soc. AIME* **239**, 119 (1967).
- <sup>4</sup>J. R. Cullen, A. E. Clark, M. Wun-Fogle, J. B. Restorff, and T. A. Lograsso, *J. Magn. Magn. Mater.* **226**, 948 (2001).
- <sup>5</sup>R. A. Kellogg, A. B. Flatau, A. E. Clark, M. Wun-Fogle, and T. A. Lograsso, *J. Appl. Phys.* **91**, 7821 (2002).
- <sup>6</sup>A. E. Clark, M. Wun-Fogle, J. B. Restorff, and T. A. Lograsso, *Mater. Trans., JIM* **43**, 881 (2002).
- <sup>7</sup>G. D. Liu, X. F. Dai, Z. H. Liu, J. L. Chen, and G. H. Wu, *J. Appl. Phys.* **99**, 093904 (2006).
- <sup>8</sup>M. C. Zhang, H. L. Jiang, X. X. Gao, J. Zhu, and S. Z. Zhou, *J. Appl. Phys.* **99**, 023903 (2006).
- <sup>9</sup>A. E. Clark, K. B. Hathaway, M. Wun-Fogle, J. B. Restorff, T. A. Lograsso, V. M. Keppens, G. Petculescu, and R. A. Taylor, *J. Appl. Phys.* **93**, 8621 (2003).
- <sup>10</sup>J. R. Cullen, A. E. Clark, M. Wun-Fogle, J. B. Restorff, and T. A. Lograsso, *J. Magn. Magn. Mater.* **226**, 948 (2001).
- <sup>11</sup>T. A. Lograsso, A. R. Ross, D. L. Schlager, A. E. Clark, and W. Wun-Fogle, *J. Alloys Compd.* **350**, 95 (2003).
- <sup>12</sup>T. A. Lograsso and E. M. Summers, *Mater. Sci. Eng., A* **416**, 240 (2006).
- <sup>13</sup>G. E. Bacon, in *Neutron Diffraction* (Clarendon, Oxford, 1975), pp. 39–40.
- <sup>14</sup>G. Petculescu, K. B. Hathaway, T. A. Lograsso, M. Wun-Fogle, and A. E. Clark, *J. Appl. Phys.* **97**, 10M315 (2005).
- <sup>15</sup>A. C. Larson and R. B. von Dreele, *GSAS, General Structure Analysis System* (LANL, Los Alamos National Laboratory, Los Alamos, 1994).
- <sup>16</sup>N. Kawamiya, K. Adachi, and Y. Nakamura, *J. Phys. Soc. Jpn.* **33**, 1318 (1972).
- <sup>17</sup>Y. Nishino, M. Matsuo, S. Asano, and N. Kawamiya, *Scr. Metall. Mater.* **25**, 2291 (1991).